Gene expression, glycocalyx assay, and surface properties of human endothelial cells cultured on hydrogel matrix with sulfonic moiety: Effect of elasticity of hydrogel

Jing Jing Yang [a], *Yong Mei Chen* [a,b], *Takayuki Kurokawa* [a,d], *Jian Ping Gong* [a*], *Shin Onodera* [c], *Kazunori Yasuda* [c]

[a] Faculty of Advanced Life Science, Hokkaido University, Sapporo 060-0810, Japan

[b] MOE Key Laboratory for Non-equilibrium Condensed Matter and Quantum Engineering, Department of Chemistry, School of Science, Xi'an Jiaotong University, Xi'an 710049, P. R. China.

[c] Graduate School of Medicine, Hokkaido University, Sapporo 060-0810, Japan

[d] Creative Research Institution, Hokkaido University, Sapporo 001-0021, Japan

Author email address: Jing Jing Yang jjyang@sci.hokudai.ac.jp; Yong Mei Chen chenym@sci.hokudai.ac.jp; Takayuki Kurokawa kurokawa@sci.hokudai.ac.jp; Jian Ping Gong gong@sci.hokudai.ac.jp; Shin Onodera onodera@med.hokudai.ac.jp; Kazunori Yasuda yasukaz@med.hokudai.ac.jp

Corresponding authors: J. P. Gong, gong@sci.hokudai.ac.jp Tel & Fax: 81-11-706-2774.

Abstract:

We measured the gene expression, glycocalyx content, and surface properties of human coronary artery endothelial cells (HCAECs) cultured on poly(sodium p-styrene sulfonate) (PNaSS) hydrogels with various levels of elasticity ranged in 3 kPa ~ 300 kPa. We found that all HCAECs reached confluence on these hydrogels while retaining the similar expression of EC-specific markers to that on polystyrene (PS), a widely used scaffold in cell culture *in vitro*. Real-time polymerase chain reaction (PCR) and glycosaminoglycan (GAG) assay showed that the amount of EC-specific glycocalyx secreted by HCAECs cultured on PNaSS gels was higher than that cultured on PS, and it increased with an increase of gel elasticity. Furthermore, the HCAECs cultured on PNaSS gels showed excellent property against platelet adhesion and lower surface friction than that on PS. The platelet adhesion and surface friction of HCAECs cultured on PNaSS gels also depend on the elasticity of gels. The largest amount of EC-specific glycocalyx, excellent blood compatibility, and the lowest friction were observed when the elastic modulus of the gel was larger than 60 kPa. Overall, HCAECs cultured on these hydrogels have better properties than those cultured on PS scaffolds, demonstrating the PNaSS gels can be used as potential tissue engineering material for blood vessels.

Keywords:

endothelial cells; glycocalyx; hydrogels; elasticity; platelet adhesion

1. Introduction

The vascular system is a complex network of vessels connecting the heart with various organs and tissues to maintain normal function. Today, cardiovascular diseases are increasingly becoming the main cause of death all over the world, which has led to an increase in the overall economic and social burden. Therefore, there is an urgent need to make rapid advancements in vascular reconstruction. Early attempts to develop blood vessel substitutes from purely synthetic polymeric conduits leads to failure due to the formation of thrombosis [1, 2], especially in small artificial blood vessels (diameter less than 6 mm).

In the real vascular system, endothelial cells (ECs) cover the inner surface of vessels. ECs are exposed to the shear stress of blood flow which modulates their function and play a role in vascular regulation, remodeling and disease. The endothelial cells inhibit thrombosis by preventing the adhesion of the platelet or blood cell to the vessel wall, and thus allow blood to easily flow even through small blood vessels and protect against vascular diseases caused by thrombosis [3-5]. The surface properties of ECs are controlled by glycocalyx that exists on the EC surface. Glycocalyx is a highly hydrated mesh of membrane-associated glycoprotein, which consists of proteoglycans (PGs), glycosaminoglycans (GAGs), and glycoproteins [5-9]. The glycocalyx layer in muscle capillaries is reported to be about 0.5 μm thick [10]. More recent studies indicate that the glycocalyx layer thickness increases with vascular diameter, at least in the arterial system, ranging from 2 to 3 μm in small arteries [11].

However, the amount of glycocalyx on ECs cultured *in vitro*, usually on solid substrates such as polystyrene (PS), was reported to be much less than that on normal ECs *in vivo* [12]. This means that even if the ECs cultured *in vitro* are lined on to the inner surface of an artificial blood vessel, they might not exhibit the same surface properties as those of ECs in *vivo*. Therefore, an important goal in

tissue engineering has been to develop an artificial extracellular matrix (ECM) on which the cultured ECs can secret the same amount of glycocalyx as that *in vivo*. However, there have been no systematic studies on the relations among various artificial ECMs, properties of ECs cultured on these ECMs *in vitro*, and secretion of glycocalyx from the ECs.

Hydrogels are expected to be used not only as artificial ECM for repairing and regenerating a wide variety of tissues and organs but also as substitute materials to develop artificial tissues and organs, since their three-dimensional network structure and viscoelasticity are similar to those of the macromolecular-based ECM in biological tissue [13-20]. Some natural protein hydrogels, including collagen, elastin, and fibronectin, and some synthetic polymer hydrogels such as polyglycolic acid (PGA), poly(ethylene oxide) (PEO), and poly(vinly alcohol) (PVA), have been used as scaffolds for cell culture [21-29]. Our previous study showed that synthetic hydrogels with negative charges, such as poly(sodium *p*-styrene sulfonate) (PNaSS), poly(2-acrylamido-2-methylpropanesulfonic sodium) (PNaAMPS), could be used as good scaffolds for cell culture without the need of any surface modification [30-33]. Synthetic hydrogels have many advantages over natural hydrogels as biomaterials: for example, infection-free, withstand high-temperature sterilization, with controllable properties, and low cost.

In the present study, we studied on the effect of scaffolds on the ECMs of ECs cultured *in vitro*. We cultured human coronary artery endothelial cells (HCAECs) on PNaSS hydrogels with various cross-linker densities and PS scaffold, which is used as control here. The expression of EC-specific markers and the surface properties of ECs on PNaSS gels, such as the relative amount of secreted glycocalyx, the blood compatibility, were compared with that on PS. Furthermore, the effect of the elasticity and the swelling degree of the gels on properties of ECs was studied. Besides that, as a method to characterize the surface of the ECs, the sliding friction of the ECs against glass substrate was also performed. As a result, HCAECs cultured on these hydrogels have better surface properties

than those cultured on PS scaffold. Our results may contribute significantly to the design of artificial blood vessels that can potentially be used in tissue engineering in future.

2. Materials and methods

2-1. Hydrogels

2-1-1. Materials

Sodium *p*-styrene sulfonate (NaSS) and *N,N′*-methylenebis-(acrylamide) (MBAA; Tokyo Kasei Kogyo, Tokyo, Japan) were purified by recrystallization from ethanol. 2-Oxoglutaric acid (Wako Pure Chemicals, Osaka, Japan), 4-(2-hydroxyethyl) piperazine-1-ethanesulfonic acid sodium salt (HEPES; Sigma, St. Louis, MO), phenol red (Sigma, St. Louis, MO), sodium chloride, and sodium hydrogen carboxyl (Junsei chemicals, Tokyo, Japan) were used as purchased. A 24-well PS tissue culture dish (Iwaki & Co., Ltd., Tokyo, Japan) was also used.

2-1-2. Synthesis

The chemical structure of PNaSS is shown in Scheme 1. PNaSS hydrogels were synthesized by radical polymerization as previously described [30, 34]. Sheets of the gels that were 1 mm in thickness were synthesized in the reaction cells. A 1 M aqueous solution of monomer (NaSS), 4–15 mol % crosslinker (MBAA), and 0.1 mol% initiator (2-oxoglutaric acid) were added to the reaction cells. After purging with nitrogen gas for 30 min, the cells were irradiated with UV light for polymerization (6 h).

After polymerization, the gels were separated from the glass plates and immersed in a large amount of deionized water for 1 week. The water was changed twice daily to remove the unreacted residual chemicals. The gels were then immersed in 4-(2-hydroxyethyl) piperazine-1-ethane sulfonic acid sodium salt (HEPES) buffer solution (HEPES 5×10^{-3} M; $NaHCO_3$, 1.55×10^{-2} M; NaCl, 0.14 M; pH 7.4). Phenol red (2.5×10^{-3} g/L) was used to visually indicate the pH of gel. After reaching

equilibrium, the pH and ionic strength of the solution containing the gels were adjusted to 7.4 and approximately 0.15 M, respectively. The thickness of the equilibrated gels was about 1.5-2 mm. The gel disks were punched out of the gel plates by a hole punch with a radius of 7.5 mm. Then after sterilizing in an autoclave (120 °C, 20 min), the gel disks were placed in a 24-well polystyrene (PS) tissue culture dish for EC culture.

2-1-3. Characterization of hydrogels

The swelling degree of gel (q) is measured as the weight ratio of the gel in its equilibrated swelling state in HEPES buffer solution to that in the dry state. Hydrogels and tissues are considered as similar materials because of their soft and wet nature. However, chemically cross-linked hydrogels made of hydrophilic polymer, including PNaSS gels, is usually a simple system just consists of polymer network in random coil state and a large amount of water (usually more than 80wt% of the total weight). The dynamic moduli G' and G'' of such a kind of chemically cross-linked gels are almost frequency-independent over a wide frequency range (0-500 rad/s). Furthermore, G''/G'= tan (δ) <<0.1 (loss angle δ<<5°) [35]. So a chemically cross-linked hydrogel can be considered as an elastic material. The elastic modulus of the PNaSS gels that equilibrated in HEPES buffer solution was characterized by compressive stress-strain measurements using a compressive tester (Tensilon RTC-1310A; Orientec Co.) [36]. For compression, samples were cut into disk (9 mm in diameter and about 2 mm in thickness), set on the lower plate of the tester, and then compressed, unconfined at the lateral direction, by the upper plate at a strain rate of 10% min^{-1} at room temperature. The elastic modulus E was determined by the average slope from a strain of 0 to 0.1 in the stress-strain curve. A representative force/displacement curve is shown in Figure S-1 of supplementary information.

2-2. Cell cultivation

2-2-1. Cell seeding

Human coronary artery endothelial cells (HCAECs; Sanko Junyaku Co., Ltd., Japan) were cultured in endothelial cell medium (EBM-2MV; Sanko Junyaku Co., Ltd., Japan), containing 20% (v/v) fetal bovine serum (FBS; GIBCO BRL Life Technologies, Inc., Gaithersburg, MD). Only the cells between passages 2-5 were used. A suspension of 2.26×10^4 cells/cm^2 ECs was used to seed the surfaces of the hydrogels and polystyrene (PS) plate. The EC-loaded samples were cultured at 37 °C in a humidified atmosphere of 5% CO_2. The medium was changed every 48 h without damaging the ECs or the gels.

2-2-2. Cell proliferation

Cell morphology and proliferation on gel surfaces were monitored using a phase contrast microscope (OLYMPUS IX 71, Japan) equipped with a digital camera using 10 × objectives lens. Cell monitoring was first performed at 6h, and then monitored every 24h, until the cells proliferated to confluence. Cell number counting at these predetermined time intervals was performed using the photography. More than four independent experiment runs were performed for each kind of hydrogel. On each sample, five different areas were selected [30].

2-3. Characterization of ECs

2-3-1. Real-time polymerase chain reaction (Real-time PCR)

The ECs were cultured on hydrogel and PS scaffolds for 5 d and reached confluence. Then, the gels were removed from their original culture wells and rinsed with phosphate-buffered saline (PBS). The ECs were scraped off the surface of the hydrogels and PS scaffold with a cell culture scraper, and then treated according to the RiboPure™ Kit protocol to isolate the RNA. Reverse transcription was carried out using the PrimeScrit™ RT reagent Kit (TakaraBio, Japan). For first-strand cDNA synthesis, 125 ng RNA was used as a template in a 10-μL reaction: 125 ng total RNA, 2 μL 5×

PrimeScript™ Buffer, 0.5 μL PrimeScrip™ RT Enzyme mix I, 0.5 μL Oligo dT Primer, 0.5 μL Random 6 mers, and RNase Free dH_2O up to a total volume of 10 μL were added to a microcentrifuge tube and mixed. The mix was incubated for 37 °C for 15 min, and then heated to 85 °C for 5 s to stop the reaction. The cDNA was stored at -20 °C until required.

All primers used for real-time PCR were designed by TakaraBio (Japan). All primer sequences are detailed in Table 1 [37, 38]. All PCR reactions were performed with SYBR Premix Ex Taq™ II (TakaraBio, Ohtsu, Japan) in standard 25-μL reactions containing 2 μL cDNA, 1 μL PCR forward primer (10 μM), 1 μL PCR reverse primer (10 μM), 12.5 μL SYBR Premix Ex Taq™ II (2×), and 8.5 μL sterile distilled water. All PCR data were calculated by using the Delta Delta Ct (△△Ct) method. The data were normalized by the appropriate housekeeping 18S levels for all samples ($\triangle Ct_1 = Ct_1$ gene of interest – Ct_1 18S), and further normalized by the levels for HCAECs cultured on the PS scaffold ($\triangle Ct_0 = Ct_0$ gene of interest – Ct_0 18S) under the same conditions. The data were therefore presented as an increase/decrease in expression of a sequence relative to that of the PS control.

2-3-2. GAG assay

The relative GAG content of ECs cultured on hydrogel and PS scaffolds were measured with a Blyscan Sulfated Glycosaminoglycan Assay kit (Biocolor Ltd., Northern Ireland, UK). The ECs were cultured on the scaffolds for 5 d and reached confluence. The hydrogel was removed from their original cultured wells. The ECs on the hydrogel and PS scaffolds were rinsed off with PBS and then immersed in papain solution (125 μg/mL in PBS (pH 6.8) with 1 mM NaCl, 5 mM cysteine-HCl, and 1 mM EDTA) to digest the glycocalyx from the surface of the ECs at 60 °C for 24 h incubated in a refrigerated incubator shaker (innova™ 4330). Then, the digested solution was separated from the ECs and treated with the cationic dye dimethyl-methylene blue (DMB), which reacted with sulfate groups on GAG side chains to produce a dye-GAG complex. Finally, the relative GAG contents were quantified by a DU 7500 spectrophotometer (BECKMAN) at A656.

Since PNaSS gels also contain the sulfate group, special caution in sample preparation is needed. All of the samples of HCAECs cultured on gels should be digested completely in the buffer solution without removing the HCAECs from the surface of the gel scaffolds in this GAG assay. There was a large error in the GAG assay results when the HCAECs were removed from gel scaffolds with a lower crosslinker concentration (data are not shown here) because the weakly crosslinked polymers on the surface of the gels were probably also removed from the surface and reacted with the dye.

2-3-3. Platelet adhesion

Platelet adhesion was tested under static conditions as previously described [33, 39, 40]. Human whole blood was received from the Hokkaido Red Cross Blood Center. The blood was centrifuged at 1200 rpm for 5 min at room temperature to separate the platelet rich plasma (PRP). Then the residue was centrifuged at 3500 rpm for 10 min to separate the platelet-poor plasma (PPP). The platelet concentration was determined by a hemocytometer. The platelet density was adjusted to 1×10^5 cells/μL by mixing PRP and PPP. Then 200 μL (platelet number, 2×10^7) of the platelet suspension was loaded on the ECs that had proliferated to confluence on the PNaSS hydrogels and PS scaffold and incubated for 2 h at 37 °C.

After rinsing off the weakly adhered platelets three times with PBS (pH 7.4), the samples were fixed by immersing into 2.5 wt% glutaraldehyde in PBS for 2 h at 37 °C. Then the fixed samples were rinsed with PBS, 50% PBS, and deionized water successively. Samples were then freeze-dried and sputter-coated using a Au target (E-1010 ion sputter; HITACHI) prior to observation under a scanning electron microscope (SEM; S-2250N; HITACHI). By counting the number of adhered platelets on the sample surfaces, the platelet adhesion densities were determined. More than three independent experimental runs were preformed for each kind of sample and five different areas were selected on each sample.

2-3-4. Friction measurement

All friction tests were performed using a rheometer (Advanced Rheometric Expansion System, "ARES"; Rheometric Scientific Inc.) as previously described [41]. A disc-shaped gel sample (radius, 7.5 mm) with an EC monolayer on one side was used for the test. The bare side of the gel was glued on to the upper surface of a coaxial disk platen with cyanoacrylate, an instant adhesive (Toagosei Co., Ltd.). A square, flat glass substrate (30 mm × 30 mm) with a surface roughness R_a = 2 nm and contact angle to water of 22° was used as the opposing substrate. The glass was glued on to the bottom of a container with an inner radius of 60 mm, which served as the lower platen in parallel with the upper platen. The test sample and opposing substrate were submerged in a protein-free medium and the two surfaces were compressed against each other under a normal pressure of 3.3 kPa, which is close to the pressure exerted on capillaries (approximately 3 kPa), to avoid any damage to the cells [42, 43]. After 10 min of static loading, the opposing substrate was rotated at an angular velocity (ω) of 10^{-3}, corresponding to a sliding velocity ($v = \omega R$) is in a range of 0 ~ 7.5 × 10^{-6} m/s from the center to the edge of the disk. During the test, the temperature of the container was maintained at 37 °C. A schematic representation of friction measurement setup for the EC monolayer is shown in Fig. 1.

In the present study, a testing time of 100 s was used. Within this measurement time, more than 80% ECs remained adhering to the gel surface, which was confirmed after every test. The dynamic frictional stress is used to represent the frictional stress between the EC monolayer and glass substrate.

2-4. Statistical analysis

Data are expressed as mean ± standard deviation at least over three samples. Statistical significance was evaluated using one way analysis of variance. Values of *P < 0.05 were considered significant, and values of **P < 0.01 were considered highly significant.

3. Results and discussions

3-1. Properties of hydrogels

Fig. 2a plots degree of swelling q as a function of the crosslinker concentration in feed. The q decreases with an increase in the crosslinker concentration. Fig. 2b plots the elastic modulus E as a function of the crosslinker concentration in feed. The value of E increases with an increase in the crosslinker concentration. In the case of a common hydrogel constituted by a three-dimensional network, its swelling degree and elastic modulus are intrinsically related. Fig. 2c shows that E changes with q following the power relation of $E \sim q^{-2.87}$. The exponent value of -2.87 lies between the theoretical values for a neutral polymer gel in a good solvent of -2.25 and in a theta-solvent of -3 [44, 45]. This result indicates that in 0.15 M HEPES that has a high ionic strength, the osmotic pressure exerted by the dissociated counter-ions of the PNaSS gels is completely screened and the polyelectrolyte PNaSS gels behave as neutral ones in terms of their water content and elasticity. The universal relation between E and q (inverse of polymer content), $E \sim q^{-2.87}$, stands for the intrinsic soft and wet nature of a hydrogel. Therefore, hereafter, we use the parameter E (or q), instead of the crosslinker concentration, in the following discussion.

3-2. HCAEC proliferation

3-2-1. Morphology

Morphology of HCAECs cultured for 120 h on PNaSS hydrogels with various E and on a PS scaffold are shown in Fig. 3. It can be seen that the HCAECs can adhere, proliferate, and reach confluence on these scaffolds. The morphology is round when cultured on hydrogels with E of 3-40 kPa and on PS with E of 3 GPa. However, the morphology is spindle when cultured on hydrogels with E of 60-300 kPa. In other words, the morphology is round on the very soft gel or very hard

scaffold but elliptic on the gels with intermediate elasticity. This means that the elasticity has a remarkable influence on the morphology of HCAECs. Furthermore, the cell morphology is more homogenous on the hydrogels than that on PS (Fig. 3).

It is worth noting that the ECs cultured on PS scaffold are easy to be removed from the PS scaffold with treatment of 0.25% trypsin/EDTA solution, but ECs could not be removed from the hydrogel scaffolds even with a higher concentration of trypsin. There are two reasons could be responsible for this phenomenon. 1) trypsin looses its activity due to adsorption to hydrogels; 2) the adhesion of the ECs to the hydrogels is stronger than that to PS, because the cells may invade into hydrogles due to its soft & wet properties. Further research is required in future to clarify the phenomenon.

3-2-2. Proliferation kinetics

The HCAECs proliferation kinetics was studied over a long-term period on the various hydrogel scaffolds. The densities of the HCAECs on PNaSS gels with different elasticity are plotted as a function of the culture time in Fig. 4. The density at 6 h is similar on all these hydrogel scaffolds, in the range of 1.75-2 × 10^4 cell/cm^2. The cell density on all gels increased with the culture time at almost the same proliferation rate, except for the PNaSS gel with E = 100 kPa, which showed a slightly higher proliferation rate from 24 to 72 h. The HCAECs cultured on all gel scaffolds reached confluence after 120 h and the cell densities were not obviously different. The final density was about 1.25 × 10^5 cell/cm^2 on all PNaSS gels.

3-3. Biological analysis of HCAECs

3-3-1. Gene expression

(1) Expression of EC-specific markers

Two relative RNA levels of EC-specific markers, vascular endothelial-cadherin (VE-cadherin)

that is an intercellular adhesion protein (Fig. 5a), and kinase insert domain-containing receptor(KDR) that is a vascular endothelial growth factor receptor (Fig. 5b), were determined by real-time PCR [38]; the results are normalized by those cultured on PS.

As shown in Fig. 5, expression of both EC-specific markers was observed for the HCAECs cultured on the gel scaffolds. The relative RNA expression for the two EC-specific markers were similar to those on the PS control, varied slightly with *E* on PNaSS gels except for the expression of VE-cadherin that is a little lower on the harder PNaSS gels than that on the PS control. This implies that HCAECs cultured on the softer PNaSS gels well retain the EC-specific property, similar to those on PS scaffold that is widely used as scaffold in cell culture *in vitro*.

(2) Expression of EC-specific glycocalyx proteins

The EC surface, *in vivo*, is covered by a hair-like layer of glycocalyx with a thickness of 0.5–3 μm, which exceeds by far that of the ECs itself (0.2 μm) [4, 6, 7]. The glycocalyx contains a large amount of PGs, in which the main components are heparan sulfate PGs (HSPGs; 50-90%), which consist of a core protein and heparan sulfate-type GAG. To investigate the effect of the gel scaffold on the glycocalyx, we determined the relative RNA levels of core proteins in HSPGs in the glycocalyx of ECs by using real-time PCR.

There are five distinct HSPG core proteins in ECs: perlecan, syndecan-1, syndecan-2, syndecan-4, and glypican [37]. In this study, all of them were found in the HCAECs cultured on the various hydrogel and PS scaffolds. A large amount of perlecan, syndecan-4, and glypican was found compared with the amount of syndecan-1 and syndecan-2 found in all HCAECs (data are not shown here). Furthermore, as shown in Fig. 6, all of the relative RNA expressions of the specific core proteins in glycocalyx for HCAECs cultured on hydrogel scaffolds are higher than those on the PS control. All of the relative RNA expressions of perlecan (Fig. 6a), syndecan-4 (Fig. 6b), and glypican (Fig. 6c) increase with *E* for the hydrogels, and the highest gene expression of these core proteins on

HCAECs were found on PNaSS with *E* of 100 kPa.

The results suggest that HCAECs cultured on hydrogels secret larger amount of glycocalyx than those cultured on PS scaffold. Furthermore, the amount of glycocalyx is influenced by the elasticity of the gel scaffolds. At the RNA level, HCAECs cultured on the harder PNaSS gels promote the secretion of glycocalyx.

3-3-2. GAG assay

We further studied the relative amount of glycocalyx secreted by HCAECs by GAG assay at the expressed-protein level. In vasculature, there are three main components of the PGs in glycocalyx, each with different kinds of GAG chains. HSPGs, the most abundant component, represent roughly 50-90% of the total amount of PGs. They are followed by chondroitin sulfate PGs (CSPGs) and hyaluronan as the second and third most common, respectively. The relative amount of total HSPGs and CSPGs can be measured by the GAG assay on the basis of the interaction between a cationic dye (DMB in this assay) and the anionic sulfate group on GAG side chains to produce a dye-GAG complex. Next, we measured the relative amount of GAG in CSPGs individually by removing the HSPGs from the glycocalyx in a GAG assay. This was done using nitrous acid to react with the *N*-sulfated hexosamines of HSPGs and thus cleave the HSPGs into 2, 5-anhydromannose residues, which do not react with DMB; the proposed mechanism is shown in reference [46].

Fig. 7a shows that HCAECs cultured on PNaSS gels expressed larger amounts of total GAG from glycocalyx than those cultured on PS scaffold, except that on soft PNaSS hydrogel with *E* of 3 kPa. This is consistent with the result of real-time PCR and demonstrates again that glycocalyx production by HCAECs is regulated by the property of scaffolds. Fig. 7b shows that the relative amount of GAG in CSPGs of HCAECs is almost independent of the elasticity of these hydrogels, showing a similar value as that on PS control. This result indicates that the difference in total GAG expression on various scaffolds derived from the different amounts of HSPGs content, which is

reported as the main components of glycocalyx in ECs *in vivo*. Accordingly, the results in Fig. 7a, b suggest that the components of PGs in the glycocalyx of HCAECs cultured on hydrgels, compared to that cultured on PS, are more similar to that *in vivo*.

The results of PCR at RNA level and GAG assay at protein level indicate that HCAECs with larger amount of glycocalyx can be found on hydrogles than those on PS scaffold. Furthermore, the amount of glycocalyx secreted by HCAECs cultured on hydrogel scaffolds is influenced by the elasticity of the gel scaffolds. The HCAECs cultured on the harder PNaSS gels promote the secretion of glycocalyx.

3-4. Surface properties of HCAECs

3-4-1. Platelet adhesion

The real-time PCR and GAG assay results showed that HCAECs cultured on gels maintain large amounts of glycocalyx on their surface in comparison with those cultured on PS. Therefore, the ECs cultured on gels are expected to have the similar surface properties and functions as that of ECs *in vivo*. Accordingly, we investigated the blood compatibility of HCAECs cultured *in vitro*. As shown in Fig. 8a, a similar platelets adhesion behavior of HCAEC monolayer on softer PNaSS gels and on PS scaffold was observed. The density of platelets that adhered to the HCAEC monolayer cultured on PNaSS hydrogel with E of 3 kPa and PS control are 9.6×10^5 platelets/μm^2 and 1.01×10^6 platelets/μm^2, respectively. However, it shows very low platelets adhesion on harder PNaSS hydrogels. The density of platelets that adhered to the HCAEC monolayer cultured on PNaSS hydrogel with E of 60 kPa and 100 kPa are 1.2×10^5 platelets/μm^2 and 3×10^4 platelets/μm^2, respectively. This phenomenon was also confirmed clearly from the SEM images shown in Fig. 8b, c, d, and e. The result indicates that the platelets adhesion of HCAEC monolayer cultured on gels is affected by the property of PNaSS hydrogels. In a word, HCAECs cultured on hydrogels of optimal

modulus have an excellent function against platelets adhesion while those on PS show a poor surface function. The result is consistent with the result of vein endothelial cells cultured on hydrogels reported by our previous investigation [34, 47].

3-4-2. Surface sliding friction

Our previous research has shown that, the negatively charged polyelectrolyte brushes on hydrogel surfaces dramatically reduce the surface sliding friction against a smooth glass in aqueous medium [48-50]. It is assumed that a lubrication layer is formed at the gel-glass interface due to the osmotic repulsion between the negatively charged gel surface and the glass substrate that is also negatively charged at pH = 7.4 [50, 51]. Here, the glycocalyx in ECs is a negatively charged macromolecule that consists of a core protein and heparan sulfate-type GAG, which contains carboxyl and sulfate groups. Thus, the surface of the EC monolayer has a negative charged polymer brush layer, similar to the polyelectrolyte brushes on gels. Therefore, the surface frictional resistance between ECs and a glass substrate could be a sensitive parameter that changes with the amount of glycocalyx secreted by HCAECs. In fact, a separate study has found that the glycocalyx on human umbilical vein endothelial cells (HUVECs) cultured on PNaSS gel plays an important role in reducing the cell friction on glass substrates [41]. The frictional stress decreased when the EC monolayers were treated with TGF-β_1, which stimulates the synthesis of HSPGs (the most important component of glycocalyx) on the EC surface, whereas the frictional stress increased when the EC monolayers were treated with heparinase I, which disrupts HSPGs.

Based on the above consideration, we examine the difference in surface friction of HCAECs cultured on different hydrogels against glass substrate *in vitro*. The friction measurement was performed at a sliding velocity in a range of $0 \sim 7.5 \times 10^{-6}$ m/s from the center to the edge of the gel disk, at which, interfacial interaction plays the dominant role of the friction [52]. Fig. 9 shows the

frictional stresses of the HCAEC monolayers culture on PNaSS hydrogels as a function of the elastic modulus *E* of the gels. The frictional stress of HCAEC monolayer cultured on PNaSS hydrogels decreased from 289 Pa to 42 Pa with an increase in *E* of PNaSS gels, and the lowest value was obtained for *E* = 100 kPa. Furthermore, the frictional stresses of EC monolayer on PNaSS hydrogels were in the range of 40-60 Pa when *E* of gels is larger than 60 kPa, which means that the coefficient of friction (frictional stress / normal pressure) of ECs against glass was very small, in the range of 0.01-0.02. Here, we consider that the decrease in the friction upon increase in the E of the gel is not originated from a decreased contact area between the cell and the glass, but due to the change of the surface properties of the ECs by the following reasons: 1) Cells reached confluent on all of these gels, and the cell density on the gels were the same regardless of the gel elasticity (Fig. 4); 2) Cells were softer than the gels, and under a normal pressure (3.3 kPa) comparable to the cell stiffness (~kPa) [53, 54], the cells underwent large deformation and are completely in contact with the glass surface.

The *E* for the dramatic decrease in the frictional stress well agrees with that when spindle cell morphology begun to be observed (Fig. 3). This suggests that the morphology of HCAECs and the surface property of HCAEC monolayers are correlated. The decrease in frictional stress of ECs with an increase of *E* of PNaSS gels is also in agreement with the results that the glycocalyx secreted by ECs increased with *E* of the PNaSS hydrogels (Fig. 7). Thus, we assume that the reduction of the friction is due to an enhancement in the glycocalyx secreted from the EC surface, similar to the role of polyelectrolyte brushes that reduce the friction, as shown in [50].

3-5. Correlation between amount of glycocalyx and surface properties of ECs

From Fig.8 and Fig.9, we observe the lowest frictional stress and the lowest platelets adhesion on HCAEC monolayer cultured on hydrogels with *E* larger than 60 kPa. Also the density of platelet

adhered on the surface of HCAEC monolayer cultured on PS scaffold is higher than that on the gels. The frictional stress of HCAECs cultured on PS against glass plate could not be measured, because the ECs was detached from the PS scaffold immediately due to the weak adhesion of cells on PS and the rigidness of PS. These results are tempting to speculate that the larger amount of glycocalyx of HCAEC monolayer, the less the friction and platelet adhesion.

Accordingly, the frictional stress and the platelet adhesion on the HCAEC monolayer might strongly depend on the amount of glycocalyx in the present system as well. Fig. 10a shows the density of platelets adhered to the EC monolayer as a function of the relative quantity of perlecan. The density of platelets decreased with an increase in the relative quantity of perlecan. This shows that the large amount of glycocalyx can restrain the platelets on the surface of the ECs. Fig. 10b shows the frictional stress on ECs as a function of the relative quantity of perlecan. The frictional stress decreased with an increase in the relative quantity of perlecan. This shows that the large amount of glycocalyx led to a decrease in the frictional stress, which was in agreement with the results for platelet adhesion.

Soft tissues are either viscoelastic or poroviscoelastic materials, and usually anisotropic. Instead of the elastic modulus E, they are characterized by an Aggregate Modulus E^* which varies markedly with deformation rate and other test conditions, including whether loads are applied in tension, compression or torsion (shear). So we cannot straightforwardly relate the optimal elastic modulus (~100 kPa) of the PNaSS gel, on which ECs showed the largest amount of glycocalyx, to the stiffness of the human native artery. However, it is tempting to compare this elastic modulus with the elastic modulus of a human native artery, which is reported about 1 MPa that is 10 times high [55]. Although the hydrogel used in this study is quite elastic with very low viscose component, we therefore speculate that when the value of E reaches 1 MPa order, we may get even a higher level of glycocalyx. On the other hand, a too high stiffness (probably much higher than 1 MPa) is not

favored as indicated by the results on PS. In reality, the modulus range of a hydrogel is in 1kPa ~ MPa. Hydrogels that is mechanically strong enough to handle with usually should have a modulus higher than 1 kPa, and this determines the lower limit of the modulus. On the other hand, a high limit of MPa is determined by the density of the polymer component for a chemically cross-linked hydrogel that is amorphous in structure. So in order to obtain a hydrogel with a modulus in the order of MPa, special structures should be introduced into the gel. This will be left for a future work.

In the above discussions, we attribute all the results to the elastic modulus E of the hydrogels. As E and the swelling degree q of a gel is related intrinsically by $E \sim q^{-2.87}$ in the present case, we cannot explicitly discuss the effect of these two parameters separately. Since the swelling degree of the gel is the inverse of weight fraction of the polymer in the gel, an increase in E means an increase in the polymer fraction as well. The latter corresponds to the increase in the surface charge density of the gels in this study, which might favor the adhesion of the cells. However, we assume that in the present study, the elasticity might play the major role by the following two facts: 1) As shown in Fig. 2, the largest change in q is about 4-folds, while the largest change in E is about 100-folds. Accordingly, the largest change in the surface polymer density or charge density is $4^{2/3} = 2.5$ folds due to the change in the swelling of gels. Comparing with a 100-folds change in E, a 2.5-folds change in the surface polymer density is much smaller. 2) Previous studies on gels of various chemical structures have shown that the behavior of ECs is sensitive to the Zeta-potential of the gel which depends on the chemical structure and surface charge density of the gel [30]. It was found that the Zeta-potential of the PNaSS gels prepared at the cross-linker concentration of 4-10 mol% is almost constant, regardless the change in the swelling degree, showing a value of -20mV [30]. This fact might be attributed to the high ionic strength of the HEPES buffer solution which screens the long range interactions of the charged moieties of the gel. PNaSS gels used in the present study also prepared at the similar cross-linker concentration range (4-15 mol%), so their Zeta-potential is also

considered as a constant of -20mV.

4. Conclusions

In this study, the biological and physical properties of HCAECs cultured on the synthetic anionic PNaSS hydrogels as well as on PS were studied *in vitro*. The results showed that all the HCAECs cultured on these hydrogels with various levels of elasticity/swelling degree could retain the similar expression of EC-specific markers to that on PS control. Furthermore, HCAECs cultured on all hydrogels are more close to "natural", in terms of its surface properties such as the adhesion to platelets, than those cultured on PS control. We found that this is because the former secrete much more characteristic glycocalyx, as elucidated on both the RNA and protein level. The results also showed that the amounts of EC-specific glycocalyx secreted by HCAECs cultured on PNaSS gels depend on elasticity of gels. Finally, the blood compatibility and frictional properties of HCAECs cultured on these gels also depend on the elasticity of the gels, and show better properties than those of HCAECs cultured on a PS scaffold. Excellent blood compatibility and the lowest frictional stresses were found when the elastic modulus of the gel is larger than 60 kPa. These results mean that the PNaSS gels can be used as excellent scaffolds for ECs culture *in vitro*. The blood vessel substitute from purely synthetic polymeric conduits is easy to form thrombosis, especially in small artificial blood vessels. Here, our results show that the ECs lined on PNaSS hydrogels with an elastic modulus of 60 kPa - 100 kPa have excellent blood compatibility and low friction properties. Therefore, these PNaSS hydrogels with their inner surfaces lined by monolayer ECs might be designed as artificial blood vessel in future.

Acknowledgments

This work is supported by a Grant-in-Aid for Specially Promoted Research (No. 18002002) from the Ministry of Education, Science, Sports and Culture of Japan.

Figure and table captions

Scheme 1 Molecular structure of the polymer used in this work.

Table 1 Primers for real-time PCR

Figure 1 Schematic representation of the frictional measurement of EC monolayer cultured on hydrogels: (1) disk-shaped hydrogels (radius R = 7.5 mm), (2) HCAEC monolayer cultured on hydrogels, (3) protein-free culture medium, (4) opposing substrate (glass plate). Normal average stress, 3.3 kPa; temperature, 37 °C.

Figure 2 a) Degree of swelling (q) of PNaSS hydrogels as a function of crosslinker concentration in feed. b) Elastic modulus (E) of PNaSS hydrogels as a function of crosslinker concentration. c) Elastic modulus (E) of PNaSS hydrogels as a function of degree of swelling (q) of gels. The solid line obeys $E \sim q^{-2.87}$. Error ranges are standard deviation over three samples.

Figure 3 Phase-contrast micrographs of human coronary artery endothelial cells (HCAECs) cultured for 120 h on PNaSS hydrogels with various elastic's modulus (E), and on polystyrene (PS) scaffold. Scale bar: 100 μm.

Figure 4 HCAECs proliferation kinetics on the surface of PNaSS gel with various elastic modulus. (Δ) 3 kPa, (□) 60 kPa, (○) 100 kPa. Error ranges are standard deviation over three samples.

Figure 5 The RNA levels of EC-specific markers as a function of elastic modulus of PNaSS hydrogels. HCAECs were cultured on the surfaces of PNaSS, and PS scaffold (control). (The relative quantity in the figure is against PS. Data are shown for a) VE-cadherin and b) KDR. Error ranges are standard deviation over three samples. * $p < 0.05$ versus the samples on PS scaffold.

Figure 6 The RNA levels of ECs specific glycocalyx proteins as a function of elastic modulus of hydrogels. HCAECs were cultured on the surfaces of PNaSS, and PS (control). Data are shown for a) perlecan, b) syndecan-4, and c) glypican. Error ranges are standard deviation over three samples. ** $p < 0.01$ versus the samples on PS scaffold.

Figure 7 a) The relative amount of total glycosaminoglycan (GAG) in the glycocalyx of HCAECs cultured on the surfaces of PNaSS hydrogels. b) The relative amount of GAG in CSPGs of HCAECs cultured on the surfaces of PNaSS hydrogels. PS scaffold was used as the control. Error ranges are standard deviation over three samples. The curved line is just to guide eyes. * $p < 0.05$, ** $p < 0.01$ versus the samples on PS scaffold.

Figure 8 a) Density of platelets adhered to HCAEC monolayer cultured on PNaSS and PS as a function of elastic modulus of scaffolds. Error ranges are standard deviation over three samples. SEM images of the adhered platelets (arrows) on the HCAEC monolayer cultured on PNaSS hydrogels with different levels of elasticity b) 3 kPa, c) 60 kPa, d) 100 kPa, and e) PS scaffold with E of 3 GPa. ** $p < 0.01$ versus the samples on PS scaffold.

Figure 9 Frictional stress and frictional coefficient of HCAEC monolayers cultured on PNaSS hydrogels sliding against glass plate as a function of elastic modulus of hydrogels. The sliding velocity is in a range of $0 \sim 7.5 \times 10^{-6}$ m/s from the center to the edge of the disk. Error ranges are standard deviation over three samples.

Figure 10 Relationship between the amount of glycocalyx and the surface properties of HCAECs cultured on PNaSS (○), and PS (Δ) scaffolds. a) Density of platelets adhered to EC monolayer as a function of relative quantity of perlecan. b) Frictional stress of HCAEC monolayer as a function of relative quantity of perlecan. Replotted from Figures 6, 8 and 9. The curved line is just to guide eyes.

Figure S-1 Supplementary information: a) Compressive stress-strain curve of a representative PNaSS hydrogel. b) Elastic modulus E was determined by the average slope from a strain ratio of 0 to 0.1 in the stress–strain curve.

References

[1] Greisler H.P. Interactions at the blood/material interface. *Ann Vasc Surg* **1990**, 4(1), 98-103.

[2] Faries P.L.; Logerfo F.W.; Arora S.; Hook S.; Pulling M.C.; Akbari C.M.; et al. A comparative study of alternative conduits for lower extremity revascularization: all-autogenous conduit versus proshetic grafts. *J Vasc Surg* **2000**, 32(6), 1080-1090.

[3] Reitsma S.; Slaaf D.W.; Vink H.; van Zandvoort M.A.; oude Egbrink M.G. The endothelial glycocalyx: composition, functions, and visualization. *Pflugers Arch-Eur J Physiol* **2007**, 454(3), 345-359.

[4] Nieuwdorp M.; Meuwese M.C.; Vink H.; Hoekstra J.B.; Kastelein J.J.; Stroes E.S. The endothelial glycocalyx: a potential barrier between health and vascular disease. *Curr Opin Lipidol* **2005**, 16(5), 507-511.

[5] Van den Berg B.M.; Vink H.; Spaan J.A. The endothelial glycocalyx protects against myocardial edema. *Circ Res* **2003**, 92(6), 592-594.

[6] Pries A.R.; Secomb T.W.; Gaehtgens P. The endothelial surface layer. *Pflugers Arch-Eur J Physiol* **2000**, 440(5), 653-666.

[7] Weinbaum S.; Tarbell J.M.; Damiano E.R. The structure and function of the endothelial glycocalyx layer. *Annu Rev Biomed Eng* **2007**, 9, 121-167.

[8] Vink H.; Constantinescu A.A.; Spaan J.A. Oxidized lipoproteins degrade the endothelial surface layer: Implications for platelet-endothelial cell adhesion. *Ciculation* **2000**, 101, 1500-1502.

[9] Constantinescu A.A.; Vink H.; Spaan J.A. Endothelial cell glycocalyx modulates immobilization of leukocytes at the endothelial surface. *Arterioscler Thromb Vasc Biol* **2003**, 23(9), 1541-1547.

[10] Vink H.; Duling B.R. Identification of distinct luminal domains for macromolecules, erythrocytes, and leukocytes within mammalian capillaries. *Circ Res* **1996**, 79(3), 581-589.

[11] Van Haaren P.M.; VanBavel E.; Vink H.; Spaan J.A. Localization of the permeability barrier to

solutes in isolated arteries by confocal microscopy. *Am J Physiol Heart Circ Physiol* **2003**, 285(6), H2848-2856.

[12] Potter D.R.; Damiano E.R. The hydrodynamically relevant endothelial cell glycocalyx observed in vivo is absent in vitro. *Circ Res* **2008**, 102(7), 770-776.

[13] Yasuda K.; Kitamura N.; Gong J.P.; Arakaki K.; Kown H.J.; Onodera S.; et al. A novel double-network hydrogel induces spontaneous articular cartilage regeneration in vivo in a large osteochondral defect. *Macromol Biosci* **2009**, 9(4), 309-316.

[14] Degoricija L.; Bansal P.N.; Sontjens S.H.; Joshi N.S.; Takahashi M.; Snyder B.; et al. Hydrogels for osteochondral repair based on photocrosslinkable carbamate dendrimers. *Biomacromolecule* **2008**, 9(10), 2863-2872.

[15] Park K.M.; Joung Y.K.; Lee S.Y.; Lee M.C.; Park K.D. RGD-conjugated chitosan-Pluronic hydrogels as a cell supported scaffold for articular cartilage regeneration. *Macromol Res* **2008**, 16(6), 517-523.

[16] Yamamura N.; Sudo R.; Ikeda M.; Tanishita K. Effects of the mechanical properties of collagen gel on the in vitro formation of microvessel networks by endothelial cells. *Tissue Eng* **2007**, 13(7), 1443-1453.

[17] Weinberg C.B.; Bell E. A blood vessel model constructed from collagen and cultured vascular cells. *Science* **1986**, 231(4736), 397-400.

[18] Chupa J.M.; Foster A.M.; Sumner S.R.; Madihally S.V.; Mattew H.W. Vascular cell responses to polysaccharide materials: in vitro and in vivo evaluations. *Biomaterials* **2000**, 21(22), 2315-2322.

[19] Pieper J.S.; Hafmans T.; Veerkamp J.H.; Van Kuppevelt T.H. Development of tailor-made collagen-glycosaminoglycan matrices: EDC/NHS crosslinking, and ultrastructural aspects. *Biomaterials* **2000**, 21(6), 581-593.

[20] Charulatha V.; Rajaram A. Influence of different crosslinking treatments on the physical

properties of collagen membranes. *Biomaterials* **2003**, 24(5), 759-767.

[21] Lin W.C.; Yu D.G.; Yang M.C. Blood compatibility of novel poly(gamma-glutamic acid)/polyvinyl alcohol hydrogels. *Colloids and Surf B Biointerfaces* **2006**, 47(1), 43-49.

[22] Terada S.; Yoshimoto H.; Fuchs J.R.; Sato M.; Pomerantseva I.; Selig M.K.; et al. Hydrogel optimization for cultured elastic chondrocytes seeded onto a polyglycolic acid scaffold. *J Biomed Mater Res A* **2005**, 75(4), 907-916.

[23] Aufderheide A.C.; Athanasiou K.A. Comparison of scaffolds and culture conditions for tissue engineering of the knee meniscus. *Tissue Eng* **2005**, 11(7-8), 1095-1104.

[24] Kue C.K; Ma P.X. Maintaining dimensions and mechanical properties of ionically crosslinked alginate hydrogel scaffolds in vitro. *J Biomed Mater Res A* **2008**, 84A(4), 899-907.

[25] Hynes S.R.; Rauch M.F.; Bertram J.P.; Lavik E.B. A library of tunable poly(ethylene glycol)/poly(L-lysine) hydrogels to investigate the material cues that influence neural stem cell differentiation. *J Biomed Mater Res A* **2009**, 89A(2), 499-509.

[26] Nolan C.M.; Reyes C.D.; Debord J.D.; Garcia A.J.; Andrew Lyon L. Phase transition behavior, protein adsorption, and cell adhesion resistance of poly(ethylene glycol) cross-linked microgel particles. *Biomacromolecules*, **2005**, 6(4), 2032-2039.

[27] Stachowiak A.N.; Irvine D.J. Inverse opal hydrogel-collagen composite scaffolds as a supportive microenvironment for immune cell migration. *J Biomed Mater Res A* **2008**, 85A(3), 815-828.

[28] Yamaguchi N.; Kiick K.L. Polysaccharide-Poly(ethylene glycol) star copolymer as a scaffold for the production of bioactive hydrogels. *Biomacromolecules*, **2005**, 6(4), 1921-1930.

[29] Kim J.; Lee K.W.; Hefferan T.E.; Currier B.L.; Yaszemski M.J.; Lichun Lu L. Synthesis and evaluation of novel biodegradable hydrogels based on poly(ethylene glycol) and sebacic acid as tissue engineering scaffolds. *Biomacromolecules*, **2008**, 9(1), 149-157.

[30] Chen Y.M.; Shiraishi N.; Satokawa H.; Kakugo A.; Narita T.; Gong J.P.; et al. Cultivation of endothelial cells on adhesive protein-free synthetic polymer gels. *Biomaterials* **2005**, 26(22), 4588-4596.

[31] Chen Y.M.; Shen K.C.; Gong J.P.; Osada Y. Selective Cell Spreading, Proliferation, and Orientation on Micropatterned Gel Surfaces. *J Nanosci Nantechnol* **2007**, 7(3), 773-779.

[32] Chen Y.M.; Gong J.P.; Tanaka M.; Yasuda K.; Yamamoto S.; Shimomura M.; et al. Tuning of cell proliferation on tough gels by critical charge effect. *J Biomed Mater Res A.* **2009**, 88(1) 74-83.

[33] Chen Y.M.; Ogawa R.; Kakugo A.; Osada Y.; Gong J.P. Dynamic cell behavior on synthetic hydrogels with different charge densities. *Soft Matter* **2009**, 5, 1804-1811.

[34] Chen Y.M.; Tanaka M.; Gong J.P.; Yasuda K.; Yamamoto S.; Shimomura M.; et al. Platelet adhesion to human umbilical vein endothelial cells cultured on anionic hydrogel scaffolds. *Biomaterials* **2007**, 28(10), 1752-1760.

[35] Tanaka Y.; Kuwabara R.; Na Y.H.; Kurokawa T.; Gong J.P.; Osada Y. J. Determination of fracture energy of double network hydrogels. *Phys. Chem. B* **2005**, 109(23), 11559-11562.

[36] Nagayama A.; Kakugo A.; Gong J.P.; Osada Y.; Takai M.; Erata T.; et al. High mechanical strength double-network hydrogel with bacterial cellulose. *Adv Funct Mater* **2004**, 14(11), 1124-1128.

[37] Princivalle M.; Hasan S.; Hosseini G.; de Agostini A.I. Anticoagulant heparan sulfate proteoglycans expression in the rat ovary peaks in preovulatory granulosa cells. *Glycobiology* **2001**, 11(3), 183-194.

[38] Yamamoto K.; Takahashi T.; Asahara T.; Ohura N.; Sokabe T.; Kamiya A.; et al Proliferation, differentiation, and tube formation by endothelial progenitor cells in response to shear stress. *J Appl Physiol* **2003**, 95(5), 2081-2088.

[39] Tanaka M.; Motomura T.; Kawada M.; Anzai T.; Kasori Y.; Shiroya T.; et al. Blood compatible

aspects of poly(2-methoxyethylacrylate) (PMEA)－relationship between protein adsorption and platelet adhesion on PMEA surface. *Biomaterials* **2000**, 21(14), 1471-1481.

[40] Tanaka M.; Motomura T.; Kawada M.; Anzai T.; Kasori Y.; Shimura K.; et al. A new blood-compatible surface prepared by poly(2-methoxyethylacrylate) (PMEA) coating. Protein adsorption on PMEA surface. *Jpn J Artif Organs* **2000**, 29(1), 209-216.

[41] Chen Y.M.; Kurokawa T.; Tominaga T.; Yasuda K.; Yoshihito K.; Gong J.P.; et al. Friction reduction by glycocalyx of endothelial cells cultured on hydrogel. Unpublished.

[42] Kamiya A.; Bukhari R.; Togawa T. Adaptive regulation of wall shear stress optimizing vascular tree function. *Bull Math Biol* **1984**, 46(1), 127-137

[43] Hahn M.; Shore A.C. The effect of rapid local cooling on human finger nailfold capillary blood pressure and blood cell velocity. *J Physiol* **1994**, 478(11), 109-114.

[44] Obukhov S.P.; Rubinstein M.; Colby R.H. Network modulus and superelasticity. *Macromolecules* **1994**, 27(12), 3191-3198.

[45] Rubinstein M.; Colby R.H.; Dobrynin A.V.; Joanny J.F. Elastic modulus and equilibrium swelling of polyelectrolyte gels. *Macromolecules* **1996**, 29(1), 398-406.

[46] Carney S.L. Proteoglycans. Carbohydrate Analysis. *A Practical Approach* **1986**, 97-141.

[47] Chen, Y.M., Yang, J.J., Gong, J.P. Adhesion, spreading, and proliferation of endothelial cells on charged hydrogels. *J. Adhes.* Waite Collection 4, **2009**, 85(11), 839-868.

[48] Kurokawa T.; Gong J.P.; Osada Y. Substrate effect on topographical, elastic, and frictional properties of hydrogels. *Macromolecules* **2002**, 35(21), 8161-8166.

[49] Kaneko D.; Tada T.; Kurokawa T.; Gong J.P.; Osada Y. Mechanically strong hydrogels with ultra-low frictional coefficients. *Adv. Mater* **2005**, 17(5), 535-538.

[50] Ohsedo Y.; Takashina R.; Gong J.P.; Osada Y. Surface friction of hydrogels with well-defined polyelectrolyte brushes. *Langmuir* **2004**, 20(16), 6549-6555.

[51] Gong J.P.; Kagata G.; Iwasaki Y.; Osada Y. Surface friction of polymer gels 1. Effect of interfacial interaction. *Wear* **2001**, 251(1-12), 1183-1187.

[52] Gong J.P. Friction and lubrication of hydrogels—its richness and complexity. *Soft Matter* **2006**, 2, 544-552.

[53] Pesen D.; Hoh J.H. Micromechanical architecture of the endothelial cell cortex. *Biophys. J.* **2005**, 88(1), 670-679.

[54] Mathur A.B.; Truskey G.A.; Reichert W.M. Atomic force and total internal reflection fluorescence microscopy for the study of force transmission in endothelial cells. *Biophys. J.* **2000**, 78(4), 1725-1735.

[55] Couet F.; Rajan N.; Mantovani D. Macromolecular biomaterials for scaffold-based vascular tissue engineering. *Macromol Biosci* **2007,** 7(5), 701-718.

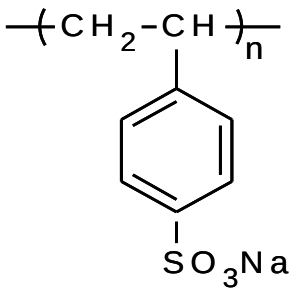

PNaSS

Scheme 1 Yang et al.

Gene	Forward	Reverse
18S	TTTGCGAGTACTCAACACCAACATC	GAGCATATCTTCGGCCCACAC
VE-cadherin	GCGACTACCAGGACGCTTTCA	CATGTATCGGAGGTCGATGGTG
KDR	AGCCAGCTCTGGATTTGTGGA	CATGCCCTTAGCCACTTGGAA
Perlecan	TCCTTGAGCTCGTCCCACAAC	GCTGGTGATGCCAAAGCAGA
Syndencan-4	AGCTGAGAGTTTATGCTGAAATGGA	TCTTGCCCAGGCAGAGATATACA
Glypican-1	CAGCTGTCCTGAACCGACTGA	TGGCACTGGCAGGGTTATTATG

Table 1

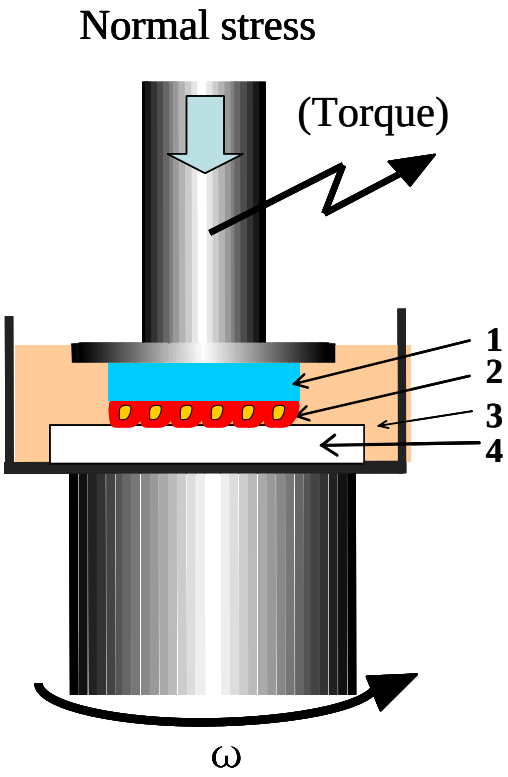

Figure 1 Yang et al.

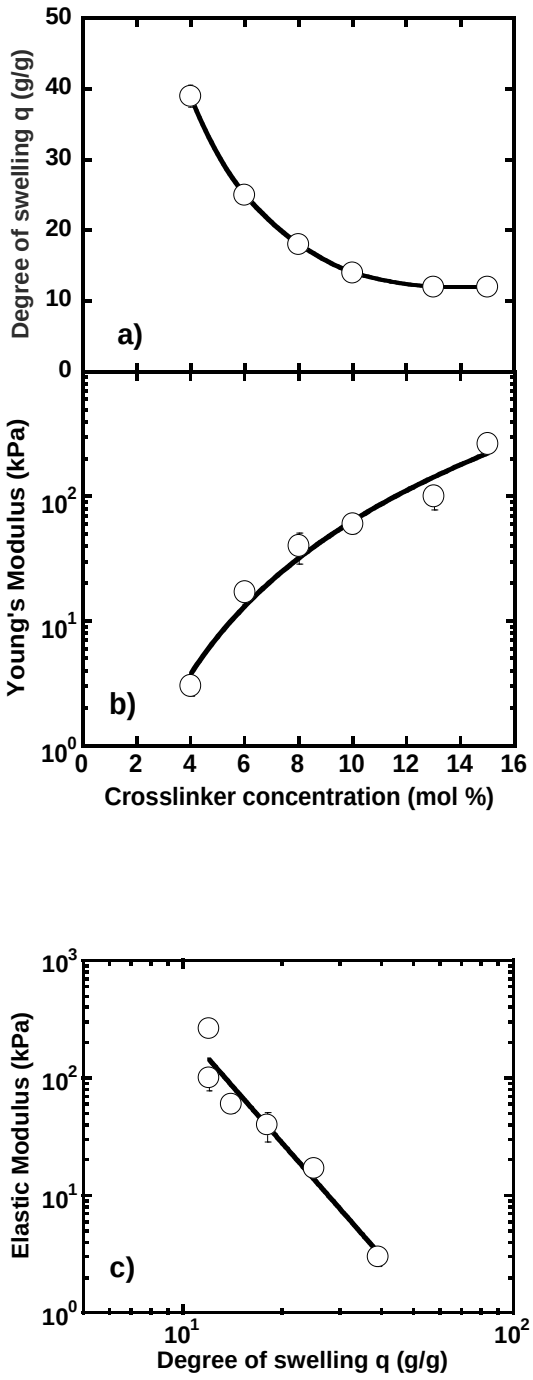

Figure 2 Yang et al.

E	
3 kPa	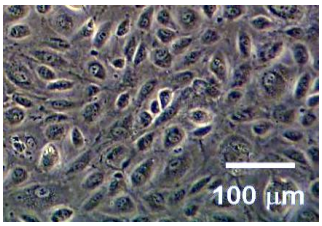
17 kPa	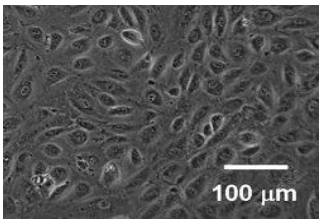
40 kPa	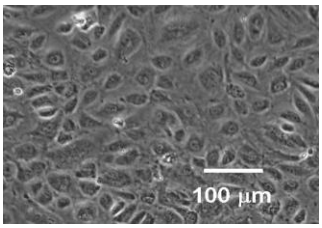
60 kPa	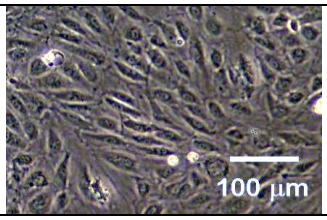
100 kPa	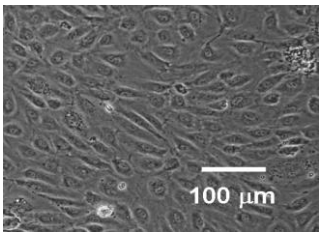
263 kPa	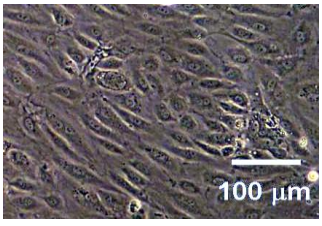
PS (control)	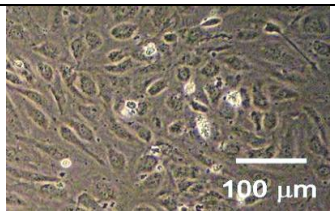

Figure 3 Yang et al.

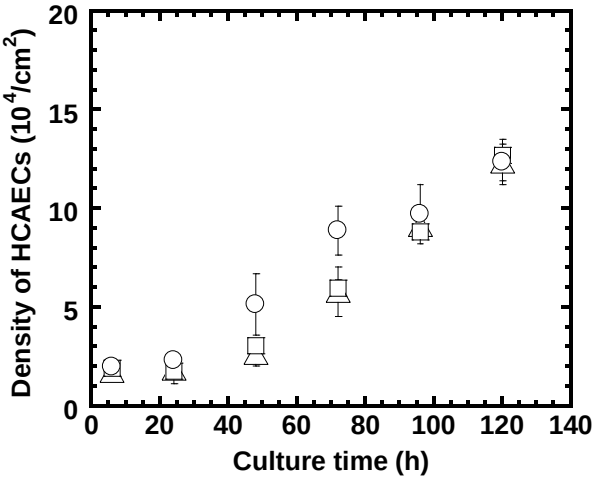

Figure 4 Yang et al.

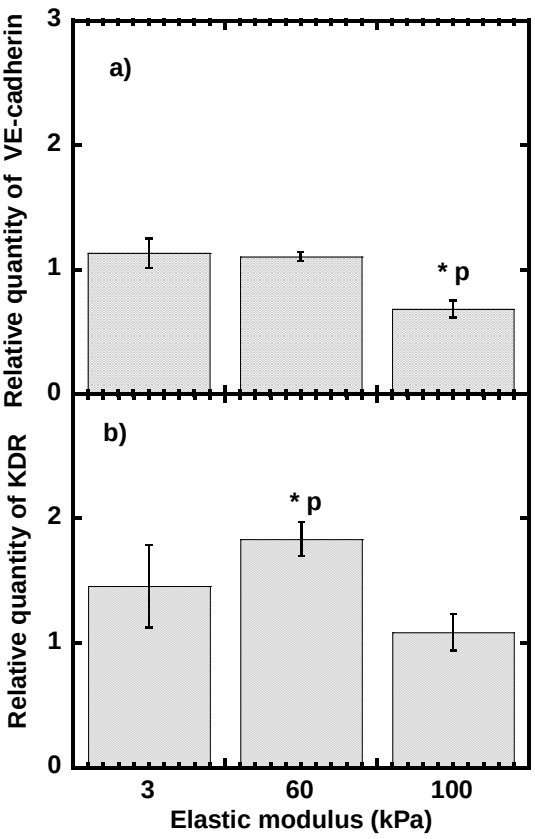

Figure 5 Yang et al.

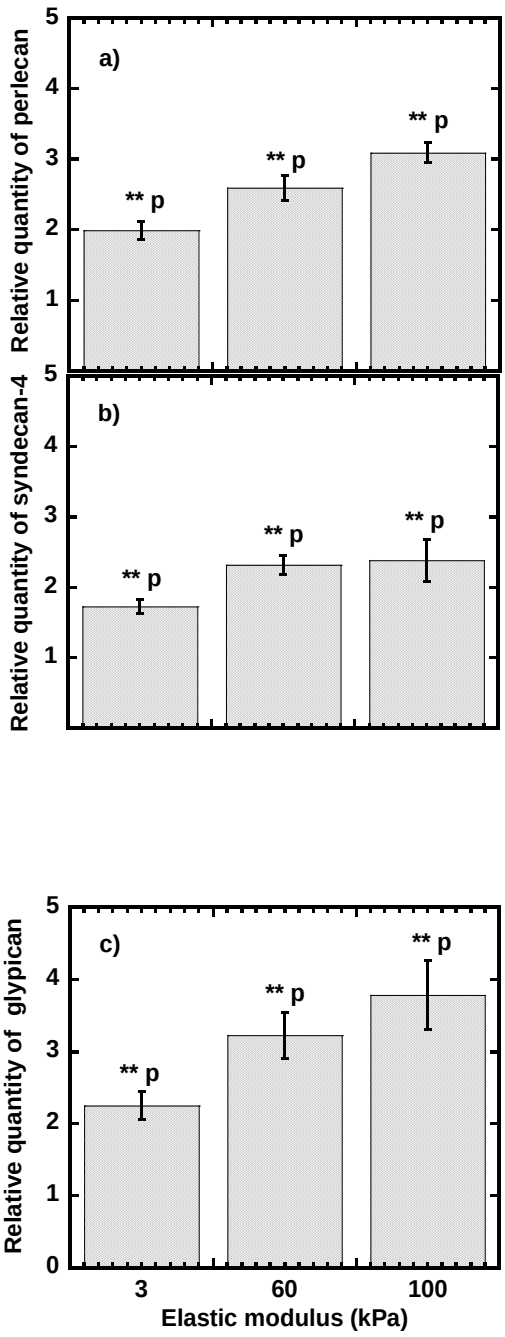

Figure 6 Yang et al.

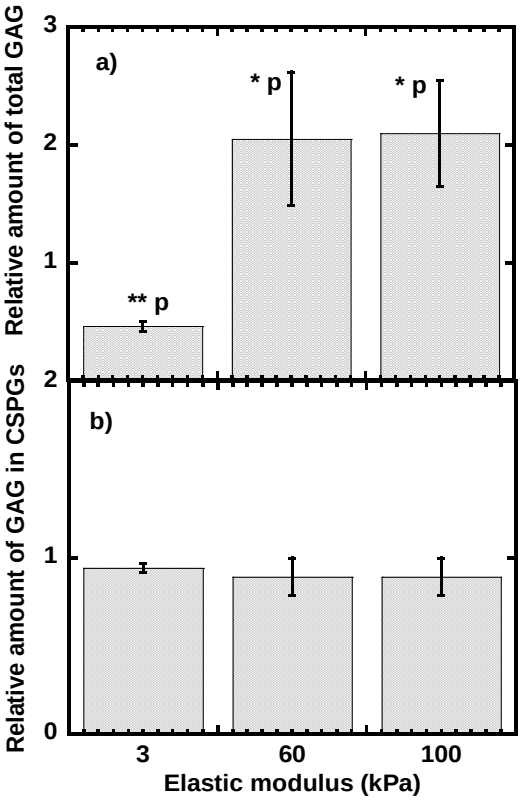

Figure 7 Yang et al.

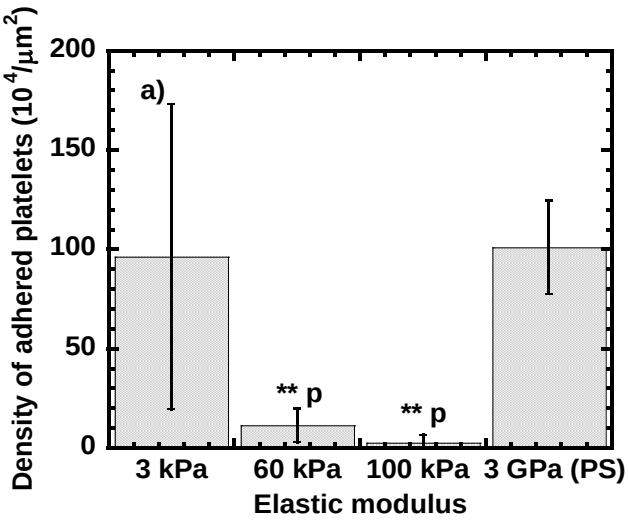

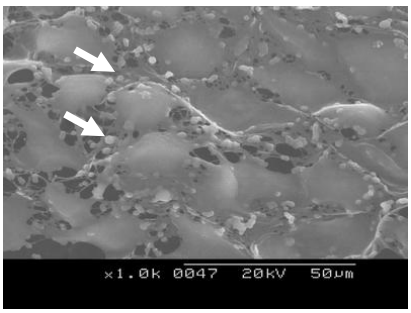

b) 3 kPa

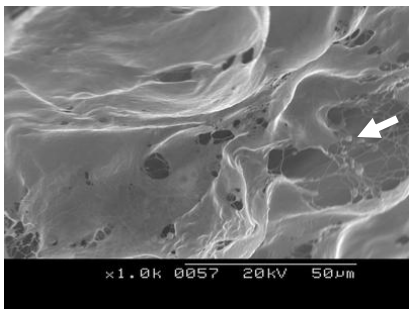

c) 60 kPa

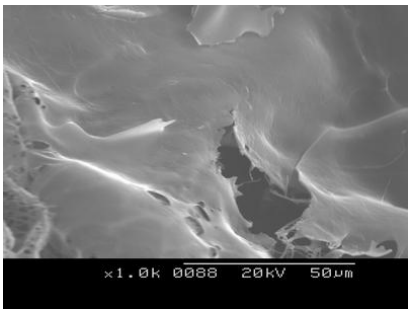

d) 100 kPa

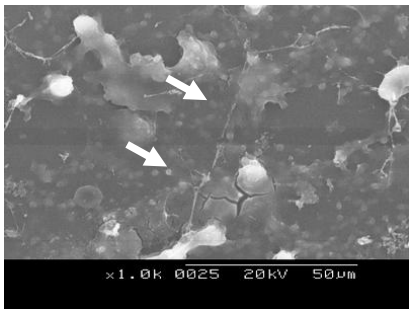

e) 3 GPa (PS)

Figure 8 Yang et al.

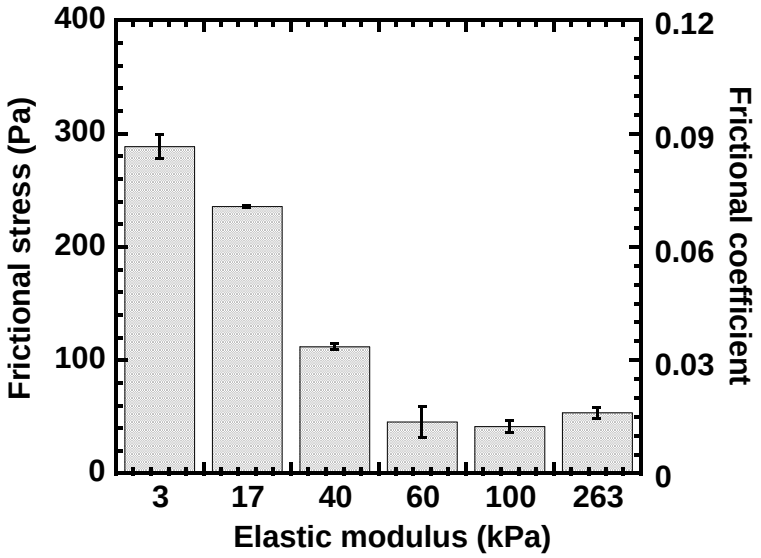

Figure 9 Yang et al.

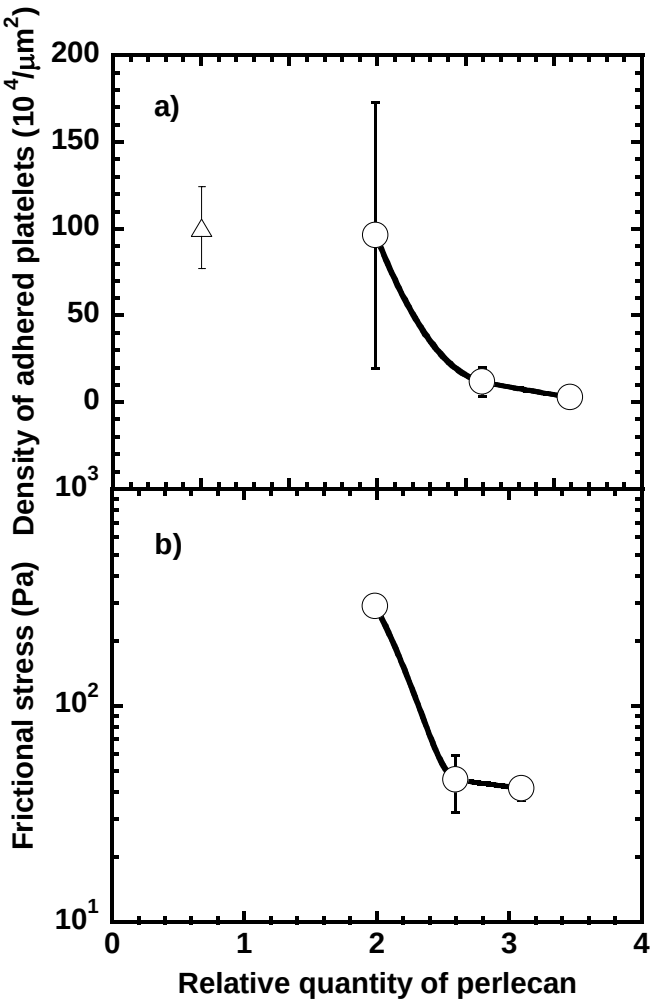

Figure 10 Yang et al.

Supplementary information

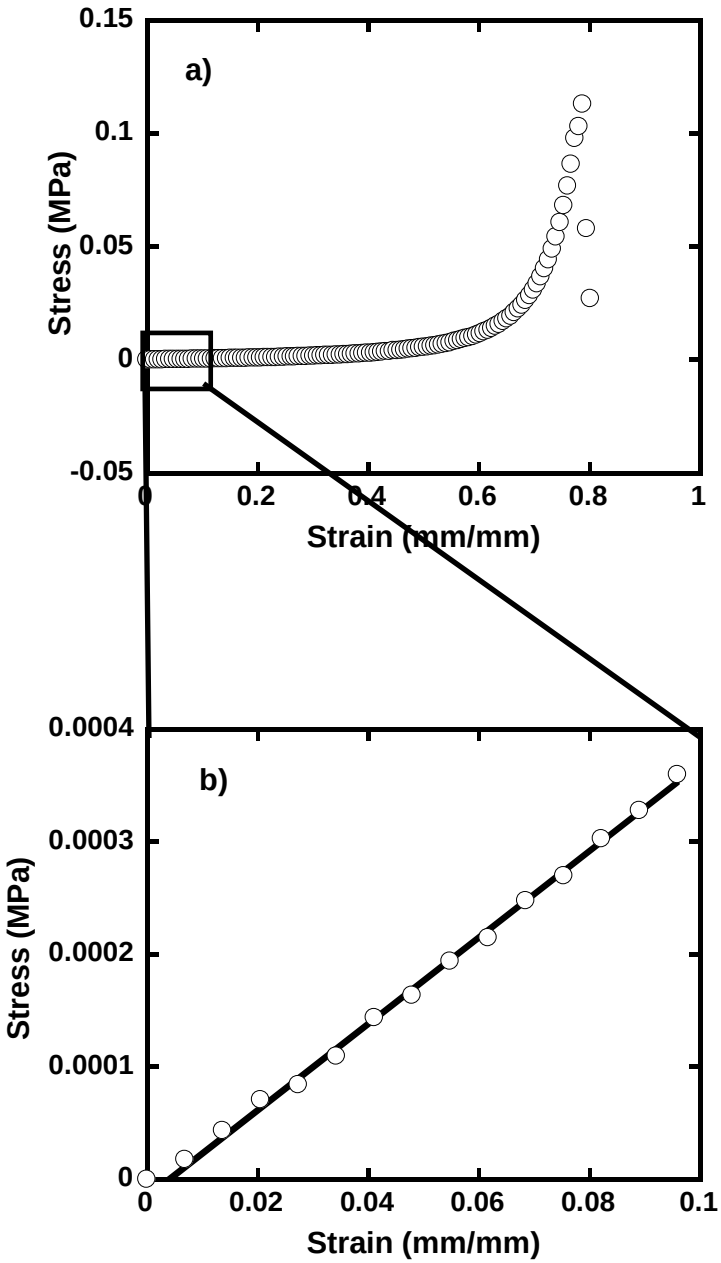

Figure S-1 Yang et al.